Microchim Acta (2010) 171:151–160
DOI 10.1007/s00604-010-0416-z

ORIGINAL PAPER

Synthesis and applications of Ce(III)-imprinted polymer based on attapulgite as the sacrificial support material for selective separation of cerium(III) ions

Jianming Pan · Xiaohua Zou · Chunxiang Li · Yan Liu · Yongsheng Yan · Juan Han

Received: 17 January 2010 / Accepted: 8 May 2010 / Published online: 30 July 2010

Abstract A surface-imprinting technique combined with a sacrificial support process was established to synthesize a novel Ce(III)-imprinted polymer (CIP) in which attapulgite acts as the sacrificial support material. The CIP was compared with attapulgite, non-imprinted polymer (NIP), and with a Ce(III)-imprinted polymer where attapulgite acts as the support material (AIP). Fourier transmission infrared spectrometry, scanning electron microscopy, transmission electron microscopy, simultaneous thermogravimetry, nitrogen sorption, and laser particle sizing were employed, and an imprinting mechanism is suggested. Batch experiments were performed to evaluate adsorption kinetics, selective recognition, adsorption isotherms, desorption and regeneration performances of the CIP. The CIP offers fast adsorption kinetics for Ce^{3+}, and the maximum adsorption capacity is 130 $mg\,g^{-1}$, which is larger than that of AIP and attapulgite. The absorption abilities of Ce^{3+} from aqueous solutions followed the order CIP>AIP>attapulgite>NIP. CIP could be reused four times with only about 16% and 18% loss of adsorption capacity in pure Ce^{3+} solution and potentially interfering ion solution, respectively. The method was applied to the separation and determination of trace Ce^{3+} in river sediments. The relative standard deviation of the method is 2.6% (n=6.0), and the detection limit (3σ) is 57 $ng\,L^{-1}$.

Keywords Attapulgite · Sacrificial support material · Surface ion-imprinted · Adsorption · Cerium(III) ions

Introduction

In the last decades, separation and enrichment technologies for cerium(III) ions (Ce^{3+}) were of interest because cerium (III) has been widely used as micro-additives functional material, gasoline catalyst, polishing powder, and in ceramic and metallurgical areas. A great deal of separation and enrichment methods for Ce^{3+} have been reported in previous work [1–4], among which solid phase extraction (SPE) was proved to be an efficient method. Then priority was given to the development of novel sorbents and to increasing their selective recognition, adsorption capacity and regeneration characteristics.

Ion-imprinting is a convenient and powerful method for synthesizing ion-imprinted polymer (IIP) which is capable of high ion recognition. The ion-imprinting process consists of polymerizing functional monomers and mixing them with template ions in the presence of a cross-linking agent. Then removal of the template ions leaves behind imprinted cavities in the polymer which provides selective binding sites for these specific template ions [5]. Because of the highly cross-linked nature of IIP, the template ions and functional groups are totally embedded inside the polymer network and the binding sites' accessibility to the template are intrinsically poor [6]. Therefore, much attention has been paid to the interesting studies of the surface-imprinting technique.

Electronic supplementary material The online version of this article (doi:10.1007/s00604-010-0416-z) contains supplementary material, which is available to authorized users.

J. Pan
School of the Environment, Jiangsu University,
Zhenjiang 212013, China

J. Pan · X. Zou · C. Li (✉) · Y. Liu · Y. Yan (✉) · J. Han
School of Chemistry and Chemical Engineering,
Jiangsu University,
Zhenjiang 212013, China
e-mail: pjm@ujs.edu.cn
e-mail: yys@ujs.edu.cn

Surface-imprinting, first proposed by Takagi's group in 1992, utilized an amphiphilic functional monomer forming a stationary complex with the template ion at the interface of the emulsion [7]. Subsequently, the surface-imprinting process based on support materials (i.e., SiO_2 [8], TiO_2 [9], α-Al_2O_3 [10], CdS [11], ZnS quantum dots [12], nanotube membrane [13], silica gel [14], magnetic Fe_3O_4 [15], etc.), which offered faster mass transfer kinetics, was established. Attapulgite is a hydrated octahedral layered magnesium aluminium silicate mineral which has siloxane groups in the bulk and silanol groups on its surface [16]. It has the potential to act as an inorganic support material in synthesizing surface-imprinting polymer because of its particular intensity, special structure, stable chemical properties and abundant raw materials.

Recently the design and synthesis of hollow functional materials combined with the surface-imprinting concept have aroused intense interest because of their novel applications in advanced separation technologies. Yilmaz et al. [17] managed to prepare spherical MIP beads by using common C4-silica particles as a sacrificial support material. He et al. [18] used a sacrificial surface molecular imprinting approach to prepare imprinted silica with testosterone as template molecule. Nearly all of these studies presented good selective recognition for target template ions over the other potentially interfering ions.

Based on the above described pioneering methods, the main purpose of this work was to present a new approach to synthesize Ce(III)-imprinted polymer (CIP) in which attapulgite acts as the sacrificial support material. During this process, attapulgite as the support material was firstly coated with a pre-polymeric ion imprinting mixture, then Ce(III)-imprinted polymer, where attapulgite acts as the support material (AIP), was obtained. In the following step, attapulgite was dissolved and removed, resulting in hollow spherical beads (i.e., CIP). Subsequently, the adsorption behaviours and separation properties of CIP, attapulgite, AIP and non-imprinted polymer (NIP) for Ce^{3+} were investigated, and the structural characteristics and imprinting mechanism of CIP were discussed in detail.

Experimental

Instruments and apparatus

Infrared spectra (4000~400 cm−1) were recorded on a Nicolet NEXUS 470 FT-IR apparatus (www.thermonicolet.com). Scanning electron microscopy (SEM) images were obtained at 15.0 kV on a Hitachi S-4800 (Hitachi, Japan) field emission scanning electron microscope (www.hitachi.com.cn). Simultaneous thermogravimetry (TG) was conducted with a NETZSCH STA 409 thermogravimetric analyzer (Bruker, USA)(www.bruker.cn). Transmission electron microscope (TEM) analysis was performed using JEOL 1200 EX at 120 keV (www.jeol.cn). The specific surface area and pore volume of the sorbents were measured according to the Brunauer-Emmett-Teller (BET) model using single point analysis and a Flowsorb II 2300 from Micromeritics Instrument Corporation, Norcross, GA (www.micromeritics.com). Measurement of the particle size of sorbents was carried out on a BIC-90 laser particle size instrument (www.bicchina.com). A Varian Liberty 150 AX Turbo model inductively coupled plasma-atomic emission spectroscope (ICP-AES) was used for the determination of Ce^{3+} from aqueous solutions (www.varian.com). The Microwave Digestion System (MDS-2003F model) was purchased from Sineo Microwave Chemisty Technology (Shanghai, China) Co., LTD (www.eu-chem.cn.ebankon.com).

Reagents and materials

A stock Ce^{3+} solution (1.0 gL^{-1}) was prepared by dissolving $Ce(NO_3)_3{\cdot}6H_2O$ (Sinopharm Chemical Reagent Co., LtdS, Shanghai, China) (www.sinopharm.com) and diluting with doubly deionised water (DDW). The standard solutions and testing solutions were prepared by appropriated dilution with DDW from the stock solution respectively. γ-glycidoxypropyltrimethoxysilane (KH-560) served as cross-linking agent (Nanjing Shuguang Chemical Group Co., China) (www.njshuguang.com). Chitosan (CTS) with 98% deacetylation and an average molecular weight of 6×104 gmol−1 (Yuhuan Biomedical Corp., China) (www.qincai.net) was used as functional monomer. Attapulgite, with an average size of 92 nm, was supplied by the Nanjing Yadong Aotu Mining Inc. in China (njydatky.cn.china.cn). Prior to use, attapulgite was activated by baking for 6.0 h at 250 °C and then dispersing in 0.1 $molL^{-1}$ NH_4Cl at room temperature. All the other chemicals used were of analytical grade, and DDW was used throughout this work.

Preparation and characterization of Ce(III)-imprinted polymer (CIP) in which attapulgite acts as the sacrificial support material

0.067 mmol CTS and 0.921 mmol Ce^{3+} were dissolved in 160 mL of 0.1 $molL^{-1}$ HAc aqueous solution. After stirring for 1.0 h, 40 mL of KH-560 was added to the mixture. Then the reaction was initiated at 25 °C and maintained at that temperature for 3.0 h while continuously stirring at 300 rpm. After that, the product was treated in an ultrasonic bath for 20 min before the activated attapulgite was added while stirring. The wet bead was allowed to evaporate at room temperature to complete the cross-linking reaction and gelation. The dry product was ground and washed with

1.0 molL^{-1} HCl and DDW to completely leach the coordinated Ce^{3+}, and then washed with 0.1 molL^{-1} $NH_3{\cdot}H_2O$ to ensure neutralization of the hydrogen ion. Then the polymer was filtered, dried at 50 °C under vacuum and ground, resulting in the desired AIP. After that, 5.0 g AIP was transferred into a screw-capped polypropylene tube and 4.0 mL of 40% aqueous HF was added while shaking the tube. The reaction was allowed to stand for 6.0 h in a water-ice bath to completely dissolve the attapulgite in AIP. Subsequently, the product was filtered and washed with 0.1 molL^{-1} $NH_3{\cdot}H_2O$ and DDW until neutrality. Then obtained CIP was dried at 50 °C under vacuum, griound and sifted with 100 meshes. For comparison, the NIP was also prepared as a blank in parallel but without the addition of $Ce(NO_3)_3{\cdot}6H_2O$.

Fourier transmission infrared spectrometry, scanning electron microscopy, transmission electron microscopy, simultaneous thermogravimetry, nitrogen sorption, and laser particle sizing were employed for the characterization of CIP.

Adsorption experiments

Adsorption of Ce^{3+} onto sorbents (i.e., attapulgite, AIP, NIP or CIP) from aqueous solutions was studied in batches. The effects of the initial Ce^{3+} concentration, pH value of the medium, quantities of sorbents, stirring time and enrichment time on the adsorption efficiency and adsorption capacity were studied. For this purpose, 50 mL aqueous solutions containing different amounts of Ce^{3+} (in the range of 0.15~20 mg) were treated with different quantities of sorbents at room temperature. Different pH ranges were adjusted with diluted HCl or $NH_3{\cdot}H_2O$. After the desired enrichment period, the concentration of Ce^{3+} in the aqueous phase was measured by ICP-AES. The main working conditions of ICP-AES are shown in Table S-1 (ESM). Finally, the percentage adsorption (E%) and adsorption capacity (Q mgg^{-1}) were calculated based on Eqs. 1 and 2, respectively.

$$E = [(C_0 - C_e)/C_0] \times 100\% \quad (1)$$

$$Q = [(C_0 - C_e)V]/W \quad (2)$$

C_0 (mgL^{-1}) and C_e (mgL^{-1}) are the initial and equilibrium concentration of Ce^{3+}, respectively. V (mL) is the solution volume and W (g) is the mass of sorbent, respectively.

Selective recognition experiments

To measure the selective recognition of CIP for Ce^{3+}, competitive metal ion recognition studies were performed. Compared with Ce^{3+}, Fe^{3+} and La^{3+} have the same charge, and La^{3+}, Pb^{2+}, Sr^{2+} have similar ionic radii, Pb^{2+} and Cs^{+} attribute to heavy metal ions and mid-low radioactive metal ions, respectively. So they were chosen as the competitive metal ions. During the experiment, Ce^{3+} and the potentially interfering ion (i.e., Fe^{3+}, La^{3+}, Pb^{2+}, Sr^{2+}, and Cs^{+}) solution, which each contained 150 μg, was transferred to a 50 mL flask. Under the optimal conditions, a certain amount of sorbent (i.e., attapulgite, AIP, CIP or NIP) was added. After adsorption equilibrium, the concentration of the non adsorbed ions in the liquid phase was determined directly by ICP-AES. The distribution and selectivity coefficients of Fe^{3+}, La^{3+}, Pb^{2+}, Sr^{2+} and Cs^{+} with respect to Ce^{3+} can be obtained from the equilibrium binding data based on Eqs. 3 and 4.

$$K_d = [(C_i - C_f)/C_f](V/W) \quad (3)$$

In Eq. 3, K_d represents the distribution coefficient; C_i (mgL^{-1}) and C_f (mgL^{-1}) represent the initial and final concentration of the metal ions, respectively; V is the volume of the solution (mL); W is the mass of sorbent (g). The selectivity coefficient (k) for the binding of a specific metal ion in the presence of competitor species can be obtained based on the following equation:

$$k = K_d\left[Ce^{3+}\right]/K_d\left[X^{m+}\right] \quad (4)$$

X^{m+} represents competitive metal ions. Comparison of the k values of the IIP (i.e., AIP and CIP) with the competitive metal ions allows an estimation of the effect of imprinting on selective recognition. A relative selectivity coefficient k' can be defined as in Eq. 5. k_s and k_n are the selectivity coefficients of CIP and NIP, respectively.

$$k' = K_c/K_n \quad (5)$$

Desorption and regeneration

Desorption of Ce^{3+} was studied with different desorption agents. The saturated CIP was placed in a desorption agent and stirred continuously at 300 rpm for 30 min at room temperature. The desorption ratio was calculated from the final Ce^{3+} concentration in the desorption agent. In order to test the regenerative capacity of the CIP, the Ce^{3+} adsorption-desorption procedure was repeated four times, using the same conditions, and the adsorption capacity of CIP in pure Ce^{3+} solution and potentially interfering ion solution was investigated in detail.

Sample preparation

The river sediments were collected from the Yudai River and Yangtse Rive, Zhenjiang, China. Each 0.2 g sediment sample was digested by microwave in the presence of 1.0 mL H_2O_2, 2.0 mL HF and 5.0 mL aqua regia. The

digested samples were immediately filtered through a Millipore cellulose nitrate membrane (pore size was 0.45 mm). Then filtrates were diluted to 100 mL and stored in polyethylene bottles.

Results and discussion

Characteristics of AIP, NIP and CIP

Analysis of structure and characteristics

FT-IR spectra of raw materials and prepared polymers are shown in Fig. 1. A wide and strong peak around 3452 cm^{-1}, from stretching vibrations of N–H and O–H in CTS, shifted to 3415 cm^{-1} and obviously became narrow in AIP before leaching the Ce^{3+} (Fig. 1e). Compared with CTS, the absorption peak of C–OH decreased from 1089 to 1074 cm^{-1} in Fig. 1e, and its shape became sharp. Moreover, a new peak at 516 cm^{-1} assigned to the Ce (III)–O appeared in Fig. 1e, but the characteristic feature of δ_sN–H at 1650 cm^{-1} and ν_{as}C–N at 1380 cm^{-1} showed no obvious change. All the above facts suggested that in the process of mixing CTS and Ce^{3+}, Ce^{3+} coordinated to −OH in CTS and formed Ce(III)–O, resulting in a CTS array around the template Ce^{3+} with a specific geometry. The matching information between $-NH_2$ in CTS and Ce^{3+} was inconspicuous. In addition, according to the Lewis Concepts of Acid and Alkali and Hard and Soft Acids and Bases from Pearson, Ce^{3+}, −OH and $-NH_2$ are hard acid, hard alkali and critical alkali, respectively. Under the acid condition, the priority is given to −OH in CTS to complete the complexation reaction with Ce^{3+}. As shown by the FT-IR spectra of AIP (Fig. 1f) and CIP (Fig. 1g), by leaching the coordinated Ce^{3+}, the absorption peak of Ce (III)–O around 516 cm^{-1} disappeared. These facts verified the conclusions mentioned above.

KH-560 is an epoxy-siloxane with trimethoxy anchor groups, and the peak for Si–O–C is at 1070 cm^{-1}. The peaks at 2960 cm^{-1} and 2840 cm^{-1} were attributed to the stretching vibrations of $-CH_3$, and the peak at 750 cm^{-1} was assigned to the epoxy group. Compared with KH-560, the peak intensity of $-CH_3$ significantly decreased, and the characteristic feature of the epoxy group vanished in AIP before adding attapulgite (Fig. 1d). Moreover, a typical Si–O–Si band around 1090 cm^{-1} was present as well. These results confirmed that KH-560 successfully linked with the complex from CTS–Ce(III) accompanied by a ring-opening process, resulting in the desired Si–O–Si network with a high degree of cross-linkage. Then, the self-condensation and co-condensation between silanols from self-hydrolysis of siloxane and attapulgite surface took place simultaneously [19]. Eventually, the overlapped absorption band of Si–O–Si from the cross-linking reaction and condensation was obtained in Fig. 1e.

When completely dissolving the attapulgite in AIP, the overlapped absorption band of Si–O–Si around 1090 cm^{-1} weakened in CIP, and the result indicated that the bonds of Si–O–Si on the surface of attapulgite were broken off successfully.

The attapulgite, AIP and CIP were all characterized using scanning electron microscopy (SEM) in order to know their surface morphological images. Moreover, a SEM image of AIP before leaching the Ce^{3+} was obtained in order to know the effect of leaching Ce^{3+} from the polymer. The SEM images are depicted as Fig. 2a–d, respectively, for attapulgite, AIP before leaching the Ce^{3+}, AIP and CIP. Compared with the attapulgite, the surface of AIP before leaching the Ce^{3+} and AIP were both ruleless and agglomerate due to coating with the products of the cross-linking and imprinting reaction. Also, it is clear that AIP displayed a slightly rough surface with many cavities by leaching template ions, and the pore size was in the nano-range, corresponding to the ion size. This indicated that a predetermined arrangement of ligands and tailored binding pockets of CIP for Ce^{3+} were left. By coordinating between Ce^{3+} and −OH in CTS, −OH was shielded in the cross-linking process, so it overcame the decrease in adsorption capacity caused by the loss of binding sites [20]. After dissolving the attapulgite, the shape of CIP

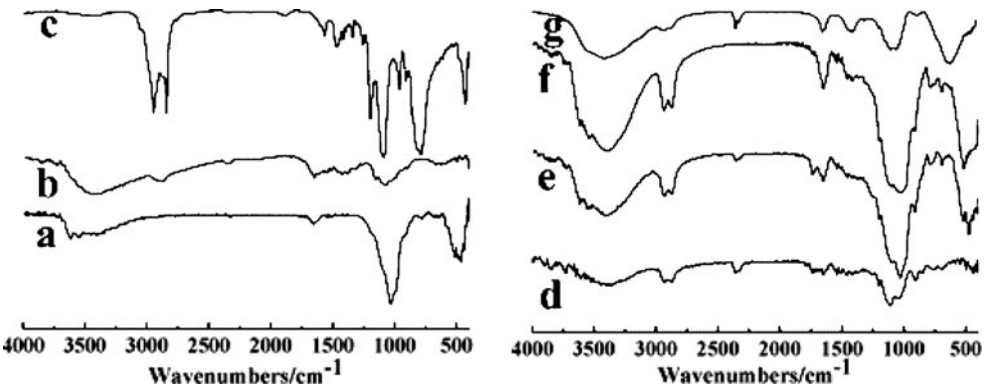

Fig. 1 FT-IR spectra of attapulgite (**a**), CTS (**b**), KH-560 (**c**), A-IIP before adding attapulgite (**d**), AIP before leaching the Ce^{3+} (**e**), AIP(f) and CIP(**g**)

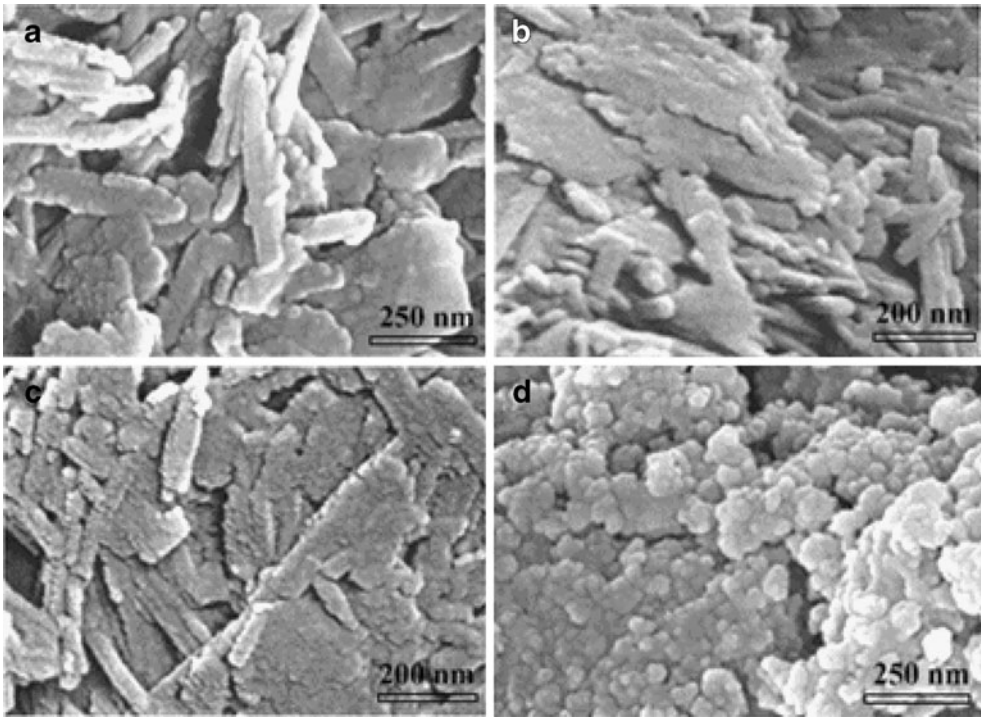

Fig. 2 SEM micrographs of attapulgite (**a**), AIP before leaching the Ce^{3+} (**b**), AIP (**c**) and CIP (**d**)

changed into a novel circle (Fig. 2d), which was different from the claval shape of AIP and attapulgite.

So as to testify the process of sacrificial support, transmission electron microscope (TEM) images (Fig. 3) and mean particle size of AIP and CIP were obtained. When compared to the claval shape for AIP (Fig. 3a), the CIP were anisomerously hollow microspheres (Fig. 3b). The mean particle size obtained for AIP was 278.4474 nm and 207.0895 nm for CIP.

Furthermore, Table S-2 (ESM) shows the surface area and pore volume for AIP, NIP and CIP. The results indicated that AIP exhibited less surface area (2.85 $m^2 g^{-1}$), which restricted its adsorption capacity as a sorbent. Along with dissolving the attapulgite in AIP with HF, because of the constriction and removal for support, the shape of CIP changed into a circle. Eventually, there was an enhancement in surface area for CIP (20.44 $m^2 g^{-1}$) due to the sacrificial-support process. Moreover, pore volumes were 0.9873, 0.9759 and 0.5374 $cm^3 g^{-1}$ for CIP, AIP and NIP, respectively. This confirmed the higher adsorption due to the Ce (III)-imprinting technique and sacrificial-support process again.

The simultaneous thermogravimetry of CIP was also studied in contrast with NIP and AIP. The results are shown in Fig. 4. The thermogravimetric curves of AIP (Fig. 4b) and CIP (Fig. 4c) were similar to two main degradation stages. The first weight loss occurred around 270 °C, which was attributed to the loss of adsorbed water molecules in the polymers. The second weight loss region (350–550 °C) with a peak at around 400 °C might be caused by the decomposition and dehydration of silanols by co-condensation. However, when the temperature

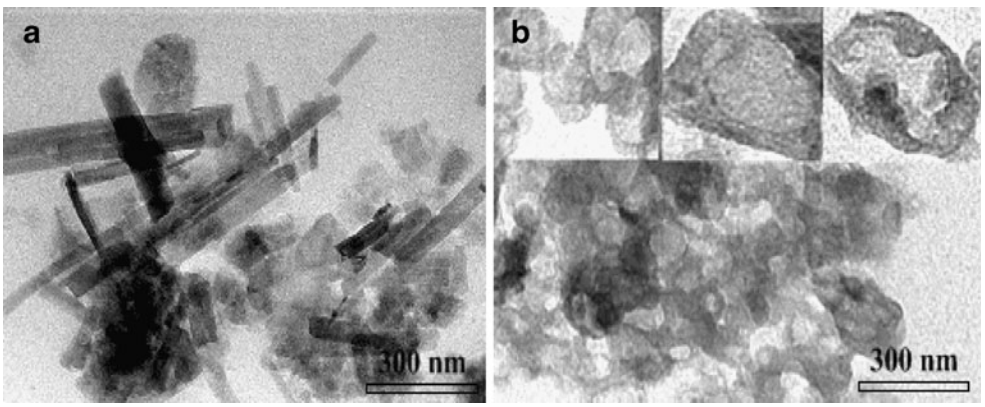

Fig. 3 TEM micrographs of AIP (**a**) and CIP(**b**)

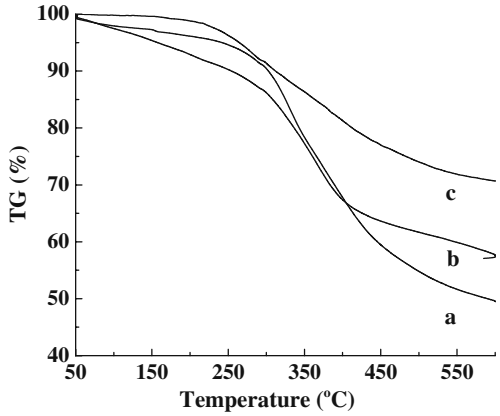

Fig. 4 TG curves of NIP (**a**), AIP (**b**) and CIP (**c**)

reached 600 °C, the weight loss ratios of AIP and CIP were 42.53% and 29.37%, respectively. Such differences might clearly indicate the effect of the sacrificial-support process. Owing to the constriction and removal for support in CIP, the density of Si–O–Si network with a high degree of cross-linkage increased, and its sizing grid became narrow. Consequently, with the enhancement of rigidity of the Si–O–Si network, the movement of big molecular chain segments was blocked. Consequently, it could be considered that the improvement in thermal stability for CIP became remarkable when the support material (i.e., attapulgite) was dissolving with HF. During the cross-linking process, the −OH and $-NH_2$ in CTS were not shielded for NIP, and they were involved with the cross-linking reaction which might lead to the absence of the inerratic Si–O–Si network for NIP. Figure 4a shows that the starting point of weight loss for NIP became a little higher than CIP, but the weight loss ratio at 600 °C was 50.80%, which was far higher than CIP.

The imprinting mechanism for Ce(III)-imprinted polymer (CIP) in which attapulgite acts as the sacrificial support material

Based on the analysis of the structure and characteristics above, the imprinting mechanism for CIP is discussed in detail. The imprinting mechanism for CIP mainly contained five steps which are shown in Fig. 5. Firstly, template Ce^{3+} was coordinated to the −OH group of the functional monomer CTS to form CTS–Ce^{3+} (Fig. 5a). In the second step, CTS–Ce^{3+} and KH-560 were present during the polymeric reaction and the cross-linked polymer network formed (Fig. 5b). Meanwhile, silanol groups were generated through acid-catalyzed self-hydrolysis of KH-560. The next step was the self-condensation and co-condensation of −OH between silanols from siloxane and attapulgite surface, then the product was grafted on the surface of attapulgite (Fig. 5c). Then, Ce^{3+} was leached from the surface of AIP, leaving behind its impression in the form of a cavity with appropriately oriented function (Fig. 5d). Finally, along with dissolving the attapulgite in AIP with the help of HF, for constriction and removal of the support,

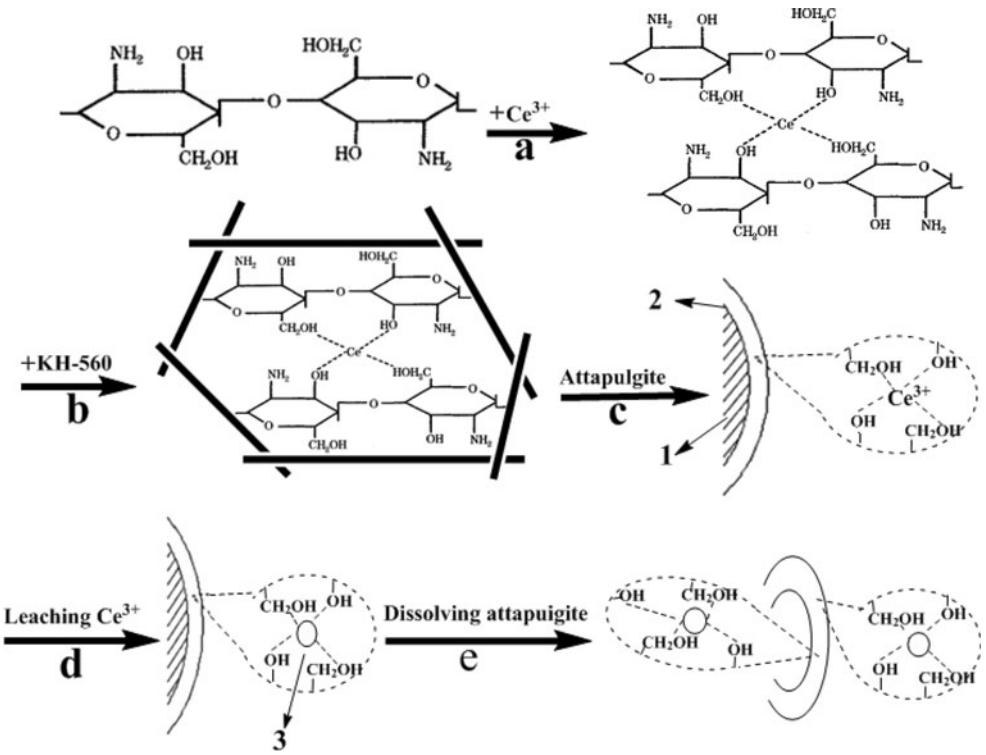

Fig. 5 Scheme of imprinting mechanism for CIP 1: attapulgite; 2: bond of Si–O–Si; 3: binding site

the shape of CIP changed into a circle, and there was an enhancement in binding sites (Fig. 5e).

Adsorption and separation of Ce^{3+} from aqueous solutions

Adsorption optimization of Ce^{3+} in the batch method

Various experimental parameters (i.e., pH, mass of sorbent, shaking time and enrichment time) were varied, and the percentage adsorption of Ce^{3+} was calculated from the results of ICP-AES. A set of solutions (50 mL volume each) was prepared, containing 150 mg of Ce^{3+}. The pH values of these solutions were adjusted between 3.0 and 5.0, and the recommend procedure was applied. Then the corresponding results were listed in Table 1. As the results indicate, when the pH value of the medium was 4.0, the weight of CIP was 0.03 g, the stirring time was 8.0 min and the enrichment time was 20 min, the percentage adsorption of Ce^{3+} reached 100%. On the other hand, without special size of the cavities and the specific binding sites with functional groups in a predetermined orientation, NIP has the lowest percentage adsorption of Ce^{3+} even under its optimal adsorption conditions. Compared with attapulgite, AIP and NIP, CIP offered the fastest kinetics for the adsorption of Ce^{3+}. Moreover, the adsorption efficiency of Ce^{3+} followed the order CIP> AIP>attapulgite>NIP.

Adsorption isotherm

The adsorption isotherms for attapulgite, AIP and CIP are shown in Fig. 6. When the equilibrium concentration increased, the adsorption capacity of CIP firstly increased sharply, then increased slightly, and finally reached a maximum point. The adsorption isotherms of attapulgite and AIP were similar in shape, and the adsorption capacity increased tardily in the whole process. The equilibrium data were then fitted to the Langmuir adsorption isotherm, assuming monolayer adsorption onto a surface with a finite number of identical sites and expressed as the following equation [21]:

$$C_e/Q_e = 1/(Q_m K_L) + C_e/Q_m \quad (6)$$

C_e is the equilibrium concentration of Ce^{3+} in solution (mgL^{-1}), Q_e is the adsorption capacity at equilibrium (mgg^{-1}), Q_m is the maximum adsorption capacity of the sorbent, and K_L represents the affinity constant.

The Langmuir adsorption isotherm constants for attapulgite, AIP and CIP are listed in Table S-3 (ESM). The experimental values of Q_m ($Q_{m,e}$) 24.41, 42.07 and 130.55 mgg^{-1} were very close to the calculated values $Q_{m,c}$ (i.e., 21.05, 38.03 and 130.23 mgg^{-1}), respectively. The highest value of K_L for CIP (0.9961 Lmg^{-1}) indicated that it has higher preference to adsorb Ce^{3+} compared to attapulgite (i.e., 0.0163 Lmg^{-1}) and AIP (i.e., 0.0312 Lmg^{-1}) by an imprinting effect and sacrificial-support process. Moreover, the correlation coefficient (r^2) values (i.e., 0.99325, 0.99845 and 0.99998) suggested that the Langmuir equation of the adsorption isotherm has reasonably high linearity.

For predicting the favourability of an adsorption system, the Langmuir equation can also be expressed in terms of a dimensionless separation factor R_L defined as follows [22, 23]:

$$R_L = 1/(1 + C_0 K_L) \quad (7)$$

Table 1 Effects of various parameters on adsorption Ce^{3+} onto attapulgite, AIP, NIP and CIP

Sorbents	pH	Adsorption (%)	Weigh (g)	Adsorption (%)	Stirring time (min)	Adsorption (%)	Enrichment time (min)	Adsorption (%)
Attapulgite	3	89.23±0.23	0.2	94.18±0.27	10	99.22±0.35	30	99.85±0.38
	4	89.35±0.15	0.25	96.39±0.34	15	99.47±0.13	40	98.90±0.24
	5*	89.67±0.25	0.3*	99.22±0.35	20*	99.85±0.38	60*	100.7±0.15
A-IIP	3	94.13±0.22	0.08	93.72±0.24	8	88.03±0.35	15	99.40±0.24
	4*	99.09±0.23	0.1	99.24±0.32	10	90.53±0.23	20	99.47±0.24
	5	98.16±0.44	0.12*	99.40±0.24	15*	99.40±0.24	30*	100.2±0.33
NIP	3	66.53±0.27	0.3	73.25±0.21	5	77.33±0.17	15	77.43±0.15
	4*	73.25±0.11	0.5	75.39±0.27	8	77.27±0.23	20	77.82±0.25
	5	72.17±0.28	0.8*	77.33±0.17	10*	77.37±0.14	30*	78.10±0.29
S-IIP	3	96.53±0.45	0.01	98.95±0.23	3	99.47±0.33	10	94.39±0.14
	4*	100.4±0.23	0.02	99.06±0.12	5	99.53±0.14	15	97.82±0.16
	5	98.37±0.12	0.03*	99.53±0.14	8*	99.78±0.22	20*	100.8±0.23

The value following"*"are the optimum conditions for the adsorption of Ce^{3+}

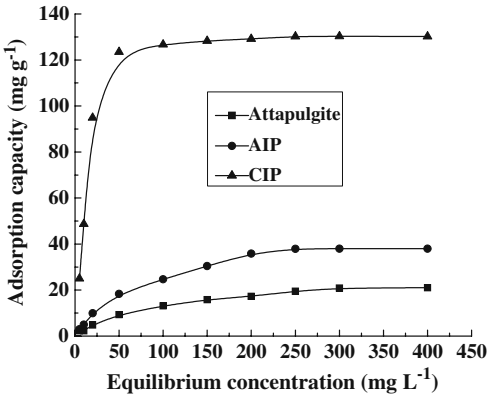

Fig. 6 Adsorption isotherms for attapulgite, AIP and CIP

When $0 R_L 1$, it represents good adsorption. Table S-4 (ESM) showed the data of R_L for adsorption of Ce^{3+}. The results indicated that the present adsorption systems were favourable for attapulgite, AIP, and CIP, and that the adsorption of Ce^{3+} was more favourable at higher initial Ce^{3+} concentration than at lower ones.

Selective recognition of Ce^{3+} from aqueous solutions

The K_d, k and k' of attapulgite, NIP, AIP and CIP for Ce^{3+} are summarized in Table 2. Due to the imprinting effect, the k values of AIP and CIP showed a more significant increase than the values of NIP. On the other hand, without the specific binding sites with functional groups in a predetermined orientation and special size of the cavities, the k values of attapulgite were also lower than those of AIP and CIP. Owing to the sacrificial-support process, along with the increase of the surface area and binding sites for CIP, there was a greater enhancement in k values than for AIP. k' is an indicator of adsorption affinity for recognition sites to the template Ce^{3+}. The results showed that the k' of the CIP was nearly 2.0–6.0 times greater than that of the NIP. Although some ions have similar radii or charge for Ce^{3+}, and some ions also have high affinity with the −OH, the CIP still exhibited high selectivity for extraction of Ce^{3+} in the presence of other metal ions. These findings indicate that the selective recognition of CIP for Ce^{3+} also followed the order CIP>AIP>attapulgite>NIP.

The competitive adsorption of metal ions onto the CIP and NIP were investigated by the batch procedure. The obtained results are exhibited in Fig. S-1(ESM). These results show that NIP has a low adsorption around 20% for each competitive metal ion. However, the CIP has specific adsorption for Ce^{3+}. So this demonstrated that the selective recognition of CIP was governed by the ionic radii and charge of original template ion, affinity between the host matrix and the guest substance [24].

Separation and analytical applications of CIP

Desorption and reuse

The regeneration of the sorbent is a key factor in improving the value in use. Desorption of Ce^{3+} from the CIP was investigated including the effects of type, concentration and volume of desorption agent. As shown in Table S-5 (ESM), the desorption study suggested that the use of 10 mL of HCl (3.0 $molL^{-1}$) for 30 min resulted in almost sufficient recovery of Ce^{3+}, which may be due to strong competitive adsorption of the hydrogen ion, demonstrating that the protonation of −OH and $-NH_2$ could prevent the adsorption of Ce^{3+}.

In order to obtain the regenerative capacity of CIP, adsorption-desorption cycles were carried out four times by using the same sorbent in batch experiments. The results (Fig. S-2) show that after four cycles of regeneration, the adsorption capacity of CIP for Ce^{3+} was about 16% loss in pure Ce^{3+} solution, about 18% loss in coexisting ion solution. The results illustrated that CIP has good regenerative capacity, even in competing metallic ion environment.

Enrichment factor

The enrichment factor is an important parameter for evaluating a sorbent, so it was studied by the recommended

Table 2 Selective recognition of the attapulgite, AIP, NIP and CIP for Ce^{3+}

Metal ions	Attapulgite		AIP		NIP		CIP		k'
	$10^4 K_d$	k	$10^4 K_d$	k	$10^4 K_d$	k	$10^4 K_d$	k	
Ce^{3+}	17.60	–	43.72	–	10.99	–	47.32	–	–
La^{3+}	7.99	2.20	11.19	3.90	5.70	1.93	6.77	6.99	3.62
Fe^{3+}	7.14	2.47	8.48	5.16	8.45	1.30	8.73	5.42	4.17
Pb^{2+}	15.44	1.14	13.32	3.28	13.04	0.84	8.07	5.87	6.96
Sr^{2+}	5.61	3.14	6.68	6.54	9.18	1.20	7.26	6.52	5.45
Cs^{+}	28.86	0.61	22.06	1.98	10.99	0.97	21.94	2.16	2.23

desorption procedure by changing the volume of sample solution and keeping the total amount of adsorbed Ce^{3+} on CIP to 150 μg. In this case, 50, 100, 150, 200, 250, 300, 350 and 400 mL of Ce^{3+} solutions were used in the adsorption-desorption procedure. When the Ce^{3+} sample volume was up to 300 mL, the recovery of Ce^{3+} could be up to 95% all the same. This may be due to strong competitive adsorption of the hydrogen ion, demonstrating that the protonation of −OH and $-NH_2$ could prevent the adsorption of Ce^{3+}. Then 300 mL of sample solution was chosen for enrichment of Ce^{3+} from sample solution. An enrichment factor of 20 was obtained because 15.0 mL of desorption agent (HCl, 3.0 molL^{-1}) was used.

Interference studies

Different amounts of potentially interfering ions were added to the mixed standard solutions containing 150 μg Ce^{3+} and adsorbed and determined according to the procedure of the adsorption experiment. Although some metal ions have similar size and charge as Ce^{3+} or high affinity to the −OH, the results exhibited in Table S-6 (ESM) show that the effects of potentially interfering ions at a given concentration are negligible. The tolerance limits of the potentially interfering ions, defined as the largest that keeps the recovery of the studied ions below 90%??, were found to be 80 mgL^{-1} for Cl^-, 60 mgL^{-1} for Na^+, 40 mg $L^{-1}K^+$, 30 mgL^{-1} for Ca^{2+}, 20 mgL^{-1} for Mg^{2+}, 16 mgL^{-1} for Ni^{2+} and Pb^{2+}, 14 mgL^{-1} for Mn^{2+}, Cd^{2+} and Hg^{2+}.

Analytical precision and detection limit

Under the optimal conditions, six portions of standard solutions were enriched and analyzed simultaneously following the general procedure. The relative standard deviation (R.S.D.) of the method was lower than 2.60%, which indicated that the method had good precision for the analysis of trace Ce^{3+} in solution samples. According to the definition from IUPAC [25], the detection limit of the method was calculated based on three times the standard deviation of 13 runs of the blank solution. The detection limit (3σ) of the proposed method was 0.057 mgL^{-1}. The calibration curve was linear within the concentration range of 0.5–8.0 mgL^{-1}. Calibration graphs obeyed the equation $A = 18.91734C(\text{mg L}^{-1}) + 0.76122 (r^2 = 0.99947)$. ($A$ is the absorbance, C is concentration of Ce^{3+} in solution and r^2 is the correlation coefficient.)

Analysis of river sediment samples

The prepared CIP was applied for the enrichment and determination of trace Ce^{3+} in two river sediment samples with the standard addition method. The recoveries were determined from spiked 0.5–3.0 mgL^{-1}, and the volume of each sample was 50 mL. The results listed in Table 3 show that the recoveries are reasonable for trace analysis in the range of 95.1%–100.8%. Evidently, the method is feasible and provides satisfactory results. The results indicate the suitability of CIP for selective separation and determination of trace Ce^{3+} in environmental samples.

Conclusions

A new type of Ce(Ш) ion imprinted polymer (CIP) was successfully prepared by the surface molecular imprinting concept combined with a sacrificial-support process, and an advanced surface-imprinting technique was developed. In the first step, Ce^{3+} imprinted composite material coating on the surface of attapulgite was carried out using Ce^{3+} as template, CTS as functional monomer and KH-560 as cross-linker. Then the attapulgite was dissolved with HF, and a novel ion imprinted polymer (CIP) was obtained. With the help of characterization, the structure characteristics and imprinting mechanism of CIP were described. It was also clear that CIP was a hollow microsphere with a greater surface area and pore volume than that of attapulgite, NIP and AIP. The adsorption experiments

Table 3 Analytical results for the determination trace Ce^{3+} in river sediment samples (n=3)

River sediment sample	Ce^{3+} added (mgL^{-1})	Concentration of Ce^{3+} (mgL^{-1})		Recovery (%)
		Found[a]	Sum	
Yudai river	0.50	0.517±0.002	1.005±0.003	97.7
	1.00		1.502±0.004	97.1
	2.00		2.504±0.002	97.5
	3.00		3.501±0.001	96.9
Yangtse Rive	0.50	0.103±0.004	0.593±0.002	90.3
	1.00		1.095±0.002	92.2
	2.00		2.099±0.003	96.1
	3.00		3.101±0.004	98.1

Volume of each sample is 50 mL

suggested that the adsorption capacity and selective recognition for Ce^{3+} also followed the order CIP>AIP> attapulgite>NIP. Furthermore, Ce^{3+} adsorption onto the CIP fitted the Langmuir model, indicating monolayer molecule adsorption. All these studies demonstrated that the preparation method was effective and the CIP was available for the selective separation of Ce^{3+} from aqueous solution.

Acknowledgments This work was financially supported by the National Natural Science Foundation of China (No.20877036).

References

1. Majdan M, Pikus S, Gladysz-Plaska A, Fuks L, Ziba E (2002) Adsorption of light lanthanides on the zeolite A surface. Colloids Surf A 209:27–35
2. Dhara S, Sarkar S, Basu S, Chattopadhyay P (2009) Separation of the ^{90}Sr-^{90}Y pair with cerium(IV) iodotungstate cation exchanger. Appl Radiat Isot 67:530–534
3. Jain VK, Handa A, Sait SS, Shrivastav P, Agrawal YK (2001) Pre-concentration, separation and trace determination of lanthanum(III), cerium(III), thorium(IV) and uranium(VI) on polymer supported o-vanillinsemicarbazone. Anal Chim Acta 429:237–246
4. Vasudevan S, Sozhan G, Mohan S, Pushpavanam S (2005) An electrochemical process for the separation of cerium from rare earths. Hydrometallurgy 76:115–121
5. Huang JH, Liu YF, Jin QZ, Wang XG, Yang J (2007) Adsorption studies of a water soluble dye, Reactive Red MF-3B, using sonication-surfactant-modified attapulgite clay. J Hazard Mater 143:541–548
6. Li Q, Su HJ, Tan TW (2008) Synthesis of ion-imprinted chitosan-TiO2 adsorbent and its multi-functional performances. Biochem Eng J 38:212–218
7. Tsukagoshi K, Yu KY, Maeda M, Takagi M (1993) Metal ion-selective adsorbent prepared by surface-imprinting polymerization. Bull Chem Soc Jpn 66:114–120
8. Ren YM, Zhang ML, Zhao D (2008) Synthesis and properties of magnetic Cu(II) ion imprinted composite adsorbent for selective removal of copper. Desalination 228:135–149
9. Wu GH, Wang ZQ, Wang J, He CY (2007) Hierarchically imprinted organic–inorganic hybrid sorbent for selective separation of mercury ion from aqueous solution. Anal Chim Acta 582:304–310
10. Chang XJ, Jiang N, Zheng H, He Q, Hu Z, Zhai YH, Cui YM (2007) Solid-phase extraction of iron(III) with an ion-imprinted functionalized silica gel sorbent prepared by a surface imprinting technique. Talanta 71:38–43
11. Birlik E, Ersöz A, Açıkkalp E, Denizli A, Say R (2007) Preconcentration of phosphate ion onto ion-imprinted polymer. J Hazard Mater 140:110–136
12. Candan N, Tüzmen N, Andac M, Andac CA, Say R, Denizli A (2009) Cadmium removal out of human plasma using ion-imprinted beads in a magnetic column. Mater Sci Eng C 29:144–152
13. Wang ZQ, Wang M, Wu GH (2010) Ion imprinted sol-gel nanotubes membrane for selective separation of copper ion from aqueous solution. Microchim Acta 169:195–200
14. Zhao JC, Han B, Zhang YF, Wang DD (2007) Synthesis of Zn(II) ion-imprinted solid-phase extraction material and its analytical application. Anal Chim Acta 603:87–92
15. Shirvani-Arani S, Ahmadi SJ, Bahrami-Samani A, Ghannadi-Maragheh M (2008) Synthesis of nano-pore samarium (III)-imprinted polymer for preconcentrative separation of samarium ions from other lanthanide ions via solid phase extraction. Anal Chim Acta 623:82–88
16. He Q, Chang XJ, Wu Q, Huang XP, Hu Z, Zhai YZ (2007) Synthesis and applications of surface-grafted Th(IV)-imprinted polymers for selective solid-phase extraction of thorium(IV). Anal Chim Acta 605:192–197
17. Yilmaz E, Ramström O, Möller P, Sanchez D, Mosbach K (2002) A facile method for preparing molecularly imprinted polymer spheres using spherical silica templates. J Mater Chem 12:1577–1581
18. He CY, Long YY, Pan JL, Li K, Liu F (2008) Molecularly imprinted silica prepared with immiscible ionic liquid as solvent and porogen for selective recognition of testosterone. Talanta 74:1126–1131
19. Li F, Jiang HQ, Zhang SS (2007) An ion-imprinted silica-supported organic–inorganic hybrid sorbent prepared by a surface imprinting technique combined with a polysaccharide incorporated sol–gel process for selective separation of cadmium(II) from aqueous solution. Talanta 71:1487–1493
20. Li F, Li XM, Zhang SS (2006) One-pot preparation of silica-supported hybrid immobilized metal affinity adsorbent with macroporous surface based on surface imprinting coating technique combined with polysaccharide incorporated sol–gel process. J Chromatogr A 1129:223–230
21. Benhammou A, Yaacoubi L, Nibou B, Tanouti B (2005) Adsorption of metal ions onto Moroccan stevensite: kinetic and isotherm studies. J Colloid Interface Sci 282:320–326
22. Huang JH, Liu YF, Jin QZ, Wang XG, Yang J (2007) Adsorption studies of a water soluble dye, Reactive Red MF-3B, using sonication-surfactant-modified attapulgite clay. J Hazard Mater 143:541–548
23. Shen W, Chen SY, Shi SK, Xiang XL, Hu WL, Wang HP (2009) Adsorption of Cu(II) and Pb(II) onto diethylenetriamine-bacterial cellulose. Carbohydr Polym 75:110–114
24. Vigneau O, Pinel C, Lemaire M (2002) Solid-liquid separation of lanthanide/lanthanide and lanthanide/actinide using ionic imprinted polymer based on a DTPA derivative. Chem Lett 2:202–204
25. Tuzen M, Citaka D, Soylak M (2008) 5-Chloro-2-hydroxyaniline–copper(II) coprecipitation system for preconcentration and separation of lead(II) and chromium(III) at trace levels. J Hazard Mater 158:137–141